
Article

Enhanced dyeing of polypropylene using fluorine–oxygen gas mixtures

Masanari Namie^{1,3}, Jae-Ho Kim^{1*}, and Susumu Yonezawa²

¹ Department of Materials Science and Engineering, Faculty of Engineering, University of Fukui, 3-9-1 Bunkyo, Fukui 910-8507, Japan; muki.namie02@gmail.com

² Cooperative Research Center, University of Fukui, 3-9-1 Bunkyo, Fukui 910-8507, Japan; yonezawa@matse.u-fukui.ac.jp

³ JAEA Tsuruga Comprehensive Research and Development Center, 1 Shiraki, Tsuruga-shi, Fukui 919-1279, Japan; namie.masanari@jaea.go.jp

* Correspondence: kim@matse.u-fukui.ac.jp

Abstract: The surface fluorination of polypropylene (PP) was performed using F₂ and O₂ gas mixtures with different F₂ gas proportions at 25 °C and 13.3 kPa for 1 h. The surface roughness of the fluorinated PP samples was approximately 1.5 times higher than that of the untreated sample (5 nm). The Fourier-transform infrared spectroscopy (FTIR) and X-ray photoelectron spectroscopy (XPS) results showed that the PP-derived bonds (-C-C- and -CH_x) decreased because they were converted into polar groups (-C-O, -CHF-, and -CF_x), which increased the surface electronegativity of PP. The variation in the F₂ gas proportion in the gas mixture significantly affected the hydrophilicity and surface composition of PP. At F₂ gas proportions of <70%, the hydrophilicity of the fluorinated PP samples improved. Notably, the hydrophilic and negatively charged PP surface enhanced the dyeing of the polymer with basic methylene blue (MB). In contrast, at F₂ gas proportions of >90%, the PP surface became hydrophobic owing to increased hydrophobic -CF₃ bonds. Thus, enhanced PP dyeing can be controlled based on the composition of the F₂ and O₂ gas mixture.

Keywords: polypropylene; surface fluorination; dyeing; zeta potential

1. Introduction

Polypropylene (PP) is an olefin polymer of great commercial importance because it is inexpensive and has many attractive physical and chemical properties [1,2]. PP, which is a saturated hydrocarbon, has a low surface energy and is categorized as a nonspecific adsorbent material. Therefore, PP has poor water wettability and very low adsorptive and adhesive properties in polar liquids [3]. Another serious disadvantage in PP dyeing is its high crystallinity and nonpolar aliphatic structure that does not possess reactive sites [4]. However, the main challenge is the absence of sites in which hydrogen bonding or electrostatic attractions can occur. To color PP, a pigment is typically added to the molten polymer before the spinning process [5]. This spin coloration of PP has been extensively used. However, this method has disadvantages such as pigment agglomeration [6] and the degradation of thermally labile dyes at the high temperatures used for resin molding. Without pigment addition, PP coloration has been investigated by staining with various dyes. Successful PP coloration depends on the surface modification of PP. For example, hydrophilic modifications, metal plating, and other coating methods are beneficial for dyeing [7–10]. Surface modification methods for hydrophilizing and roughening plastic surfaces include physical treatments, such as plasma [11], ozone [12], UV light [13], corona discharge [14], wet chemical treatments [15], and ion irradiation [16]. However, these treatments are expensive and unsuitable for complex geometries. In addition to these conventional chemical and physical methods, direct fluorination has been investigated for the

surface modification of polymers [17, 18]. This chemical method involves a gas-phase chemical reaction between fluorine gas (F_2) and the polymer surface, which effectively modifies and controls the physicochemical surface properties of polymers.

Previously, the surface of polyethylene terephthalate (PET), polycarbonate (PC), and PP were modified by direct fluorination, achieving high adhesion with plating and good dyeability [19–21]. In particular, we reported that dyeing PP with basic dyes can be improved by surface fluorination because of the increased roughness and negative charge of the surface [21]. However, in the case of direct fluorination with pure fluorine gas, the fluorinated layer formed on the PP surface contains numerous hydrophobic fluorocarbons ($-CF_3$), which prevented the wettability between PP and the staining solution, causing limited dyeability. Surface fluorination using a mixture of F_2 and O_2 gas produced a higher hydrophilic surface of PC resin, as reported previously [20]. This study aims to enhance PP dyeing using a mixture of F_2 and O_2 gas. In addition, the effects of the gas proportion of F_2 in the gas mixture on PP dyeability are investigated.

2. Materials and Methods

2.1 Surface fluorination of polypropylene

PP film was obtained from Takiron Corp. PP plates ($10 \times 10 \times 1.2$ mm) were cut and washed with ethanol to remove organic residues from the PP surface. F_2 gas (99.5% purity) was produced by electrolysis of a KF/HF mixture in an HF solution. O_2 gas (purity 99.5%) was supplied from a cylinder manufactured by Uno Sanso Co., Ltd. The PP plates were placed in a nickel reaction vessel ($24 \times 32 \times 5$ mm 3) and maintained at 25 °C under vacuum (0.1 Pa) for 10 h to eliminate impurities from the system before use. We previously described the fluorination apparatus [22], where a reaction temperature of 25 °C, total gas pressure of 13.3 kPa, and reaction time of 1 h were used. The sample names and F_2 and O_2 gas mixing ratios are summarized in Table 1. After the reaction was complete, the reaction vessel was purged with Ar gas.

Table1. Sample names and fluorination conditions.

Sample name	Gas pressure (kPa)	Gas mixture ratio (vol%)		Reaction temp. (°C)	Reaction time (Min.)
		F_2	O_2		
untreated	-	-	-	-	-
F10		10	90		
F30		30	70		
F50		50	50		
F60	13.3	60	40	25	60
F70		70	30		
F90		90	10		
F100		100	0		

2.2 Material characterization

The chemical compositions of the untreated and modified PP samples were determined by Fourier-transform infrared spectroscopy (FTIR; Nicolet 6700, Thermo Electron Scientific). FTIR analysis was conducted in the transmittance mode in the range of 650–4000 cm $^{-1}$ by acquiring 32 scans and applying air background removal. The surface

chemical states of the untreated and modified PP samples were characterized by X-ray photoelectron spectroscopy (XPS; JPS-9010, JOEL). The binding energies were referenced to a carbon peak at 285.0 eV. The surface morphologies of the untreated and modified PP samples were characterized by confocal laser scanning microscopy (CLSM; OLS5000, Olympus), and surface topography was characterized by atomic force microscopy (AFM; Nanoscope IIIa, Digital Instruments). Scanning was conducted in the tapping mode over an area of $10 \times 10 \mu\text{m}^2$. The arithmetic mean surface roughness (Ra) was determined from the AFM roughness profile. The static water contact angles of the untreated and modified PP samples were measured at 25 °C using the sessile drop method. A water droplet (10 μL) was used in a telescopic goniometer with a magnification power of 23 \times and a protractor graduation of 1° (Model 100-00-(230), Rame-Hart). To determine the average contact angle value ($\pm 2^\circ$), five measurements were acquired at different surface locations on each sample. The zeta potential profiles of the PP samples were measured on a zeta potential analyzer (EISZ-2, Otsuka Electronics Co., Ltd.) using a solid sample cell unit.

2.3 Dye staining of polypropylene

Methylene blue (MB; Hirono Pure Chemical Corp.) and acid orange 7 (O2: orange II; Nacalai Tesque, Inc.) were used as representative basic and acidic dyes, respectively. Staining solutions, prepared with 0.4 g/L of dye in ultrapure water, were placed in a water bath at 80 °C, and the PP samples were immersed for 30 min. Subsequently, the PP samples were washed with ultrapure water and air-dried. The surface staining of each sample was evaluated based on the N content, which was analyzed by XPS. Furthermore, the aromatic C=C stretching peak derived from the MB and O2 dyes in each sample was examined at 1600 cm^{-1} by FTIR.

3. Results and Discussion

3.1. Effects of fluorination using F_2 and O_2 gas mixtures on the surface morphology of polypropylene

The surface morphology and hydrophilicity of the untreated and fluorinated PP samples are shown in Figure 1. The surface morphology was characterized by CLSM and AFM. No difference in the CLSM images of the untreated and fluorinated samples was observed. The AFM image of the untreated sample showed a relatively flat and smooth surface, with a low surface roughness of $\sim 5.002 \text{ nm}$. However, the surface roughness of the fluorinated PP samples was higher than that of the untreated sample. Surface fluorination caused fine surface defects at the nanoscale level, but not at the microscale level. This is likely owing to small molecules or amorphous regions formed after fluorination, as well as CF_4 gasification. In addition, the surface roughness of the fluorinated PP samples generally increased with increasing F_2 content in the gas mixture. The surface hydrophilicity of the samples was evaluated using a water contact angle test. The water contact angle of the untreated PP sample was approximately 94°. The hydrophilicity of the PP samples fluorinated using a F_2 gas proportion of $< 70\%$ was higher than that of the untreated sample, as shown in Figure 1. In particular, the F50 sample prepared with a fluorine gas concentration of 50% was the most hydrophilic, which may be owing to its increased surface roughness. Furthermore, the partial polarity of the surface was enhanced by the addition of F, whose high electronegativity and acidity easily attracted water as a polar solvent. In contrast, the contact angle of the PP samples fluorinated using a F_2 gas proportion of $> 90\%$ was higher than that of the untreated sample, which may be owing to the formation of hydrophobic C-F₃ bonds on the PP surface.

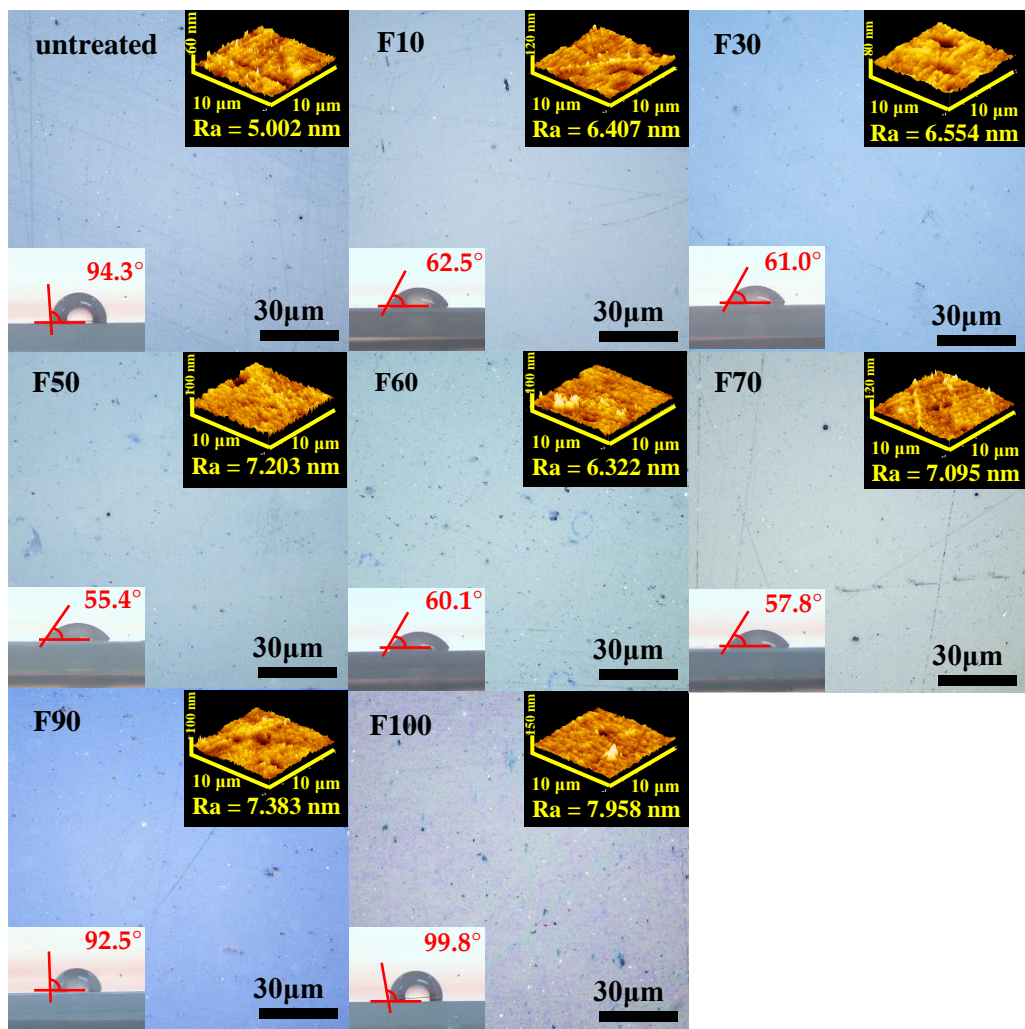


Figure 1. CLSM, AFM and contact angle measurements of untreated and fluorinated samples.

3.2 Effects of fluorination on the surface composition and structure of polypropylene

The FTIR spectra of the untreated and fluorinated PP samples are shown in Figure 2. The untreated PP sample exhibited absorption bands at 2960 and 2950 cm^{-1} ($-\text{CH}_3$, asymmetrical vibration), 2919 cm^{-1} ($-\text{CH}_2-$, asymmetrical vibration), 2867 cm^{-1} ($-\text{CH}_3$, symmetrical vibration), 2839 cm^{-1} ($-\text{CH}_2-$, symmetrical vibration), 1458 cm^{-1} ($-\text{CH}_2-$, bending vibration), and 1376 cm^{-1} ($-\text{CH}_3$, wagging vibration) [23]. After surface fluorination, new absorption bands appeared at 700–770 cm^{-1} ($-\text{CF}_3$) and 1000–1200 cm^{-1} ($-\text{CF}$, $-\text{CF}_2-$) [24], and the peak intensity of the PP bonds ($-\text{CH}_3$, CH_2) decreased. Fluorination at high F_2 gas concentrations in the gas mixture increased the intensity of the peaks associated with fluorinated bonds ($-\text{CF}$, $-\text{CF}_2$, $-\text{CF}_3$), and decreased the intensity of the peaks associated with PP. Because the $-\text{CH}_2-$ and $-\text{CH}_3$ peaks almost disappeared in the fluorinated samples with high F_2 gas concentrations, such as F90 and F100, it is thought that a fluorinated layer was formed up to the detection limit depth of several micrometers by FTIR. Moreover, the surface fluorination using the F_2 and O_2 gas mixtures introduced C=O bonds (1755 and 1850 cm^{-1}) into the PP samples, which may enhance dye adsorption. However, the intensity of the C=O peaks decreased significantly for gas mixtures with a F_2 proportion of >90%, as shown in Figure 2.

The C 1s, O 1s, and F 1s XPS spectra of the untreated and fluorinated PP samples are shown in Figure 3. The untreated PP sample exhibited strong C–C bonding at 285.4 eV, which disappeared after fluorination. These C–C bonds were converted to $-\text{C–O}$ and $-\text{C=O}$

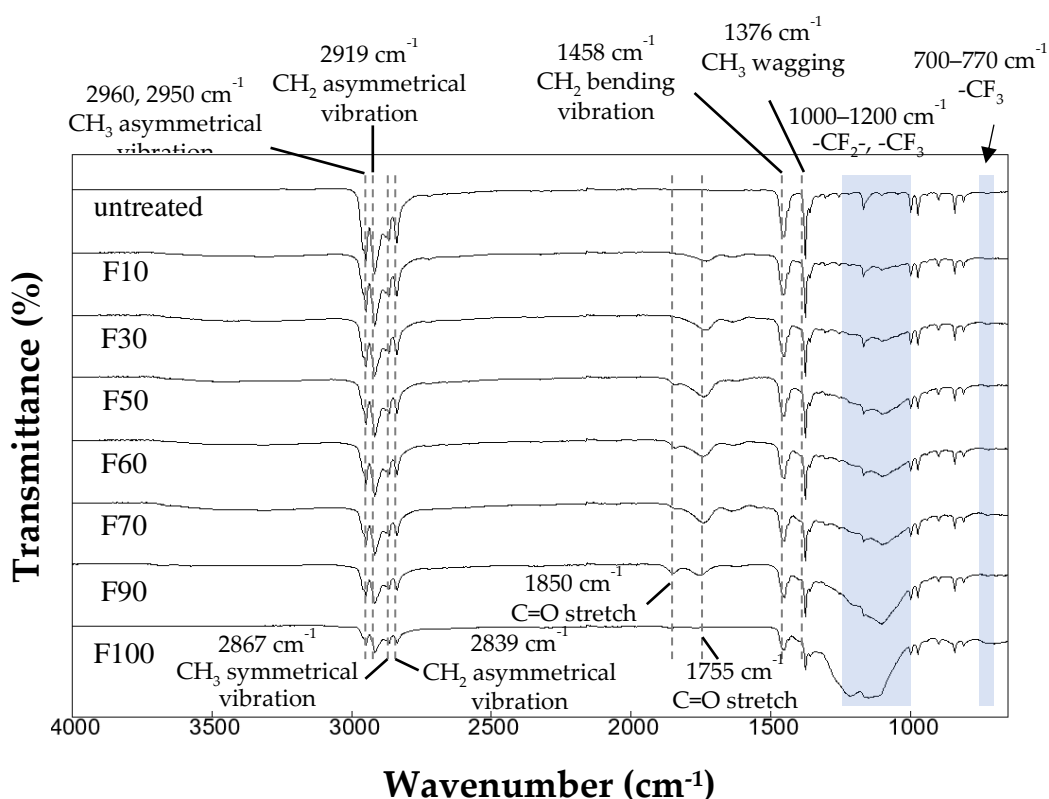


Figure 2. FTIR spectra of the untreated and fluorinated samples.

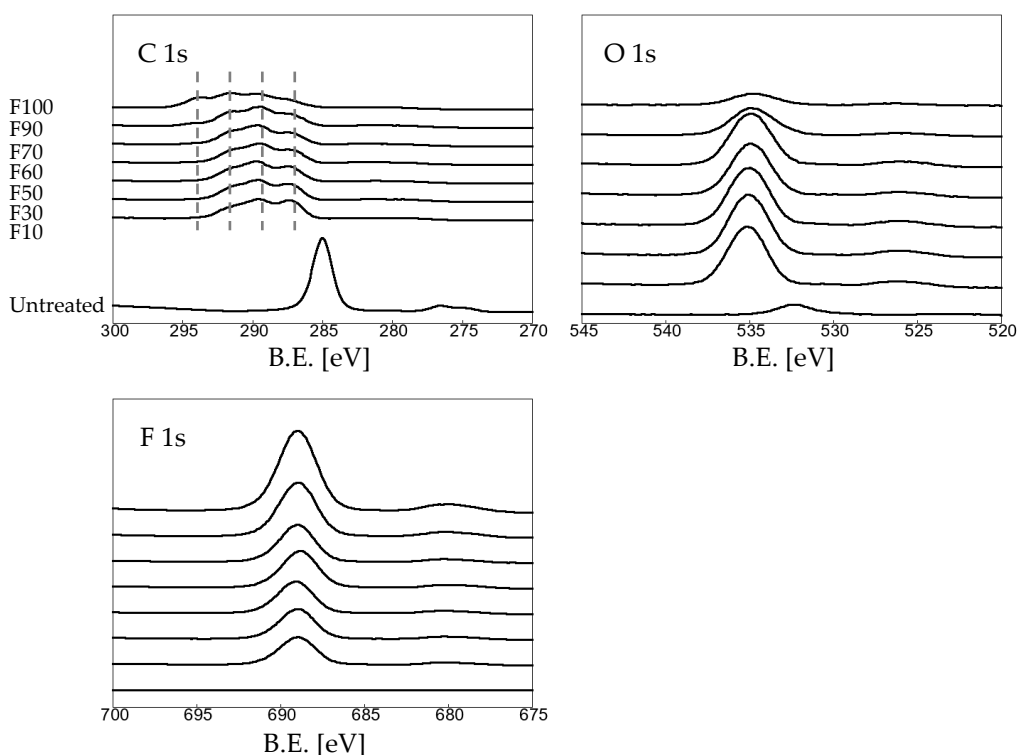


Figure 3. XPS spectra of the untreated and fluorinated samples.

bonds (287.4 eV) in the form of a $-\text{C}(=\text{O})\text{OH}$ group with water in air, which facilitates covalent dye adsorption, or to $-\text{CHF}-$ (289.5 eV), $-\text{CF}_2-$ (291.5 eV), and $-\text{CF}_3$ (294.0 eV), which serve as the main hydrogen bonding sites for water adsorption. Increasing the F_2 gas proportion in the gas mixtures resulted in an increase in the amount of polar groups ($-\text{CF}_x$). For F 1s and O 1s, increasing the F_2 gas proportion in the gas mixtures caused an increase in the F contents, whereas the O contents decreased. In particular, the trend was clearly observed for samples F90 and F100. This may be owing to the formation of stable CF_3 bonds on the sample surface, which yielded a hydrophobic surface (Figure 1).

Table 2. The elemental concentration of C, O, and F on the untreated and fluorinated PP samples determined by XPS (Figure 3).

Sample name	Elemental composition (%)		
	C 1s	O 1s	F 1s
untreated	94.52	5.45	0.03
F10	47.01	20.76	32.24
F30	45.24	21.09	33.67
F50	44.43	20.16	35.41
F60	42.11	17.50	40.39
F70	41.10	18.30	40.60
F90	38.23	8.57	53.20
F100	29.78	3.05	67.17

Table 2 shows the elemental concentration of C, O, and F on the untreated and fluorinated PP samples determined by XPS (Figure 3). Varying the F_2 gas proportion in the gas mixture influenced the elemental composition of the surface layer. With an increase in the F_2 gas proportion in the $\text{F}_2\text{-O}_2$ gas mixture, the F contents on the surface of the fluorinated PP samples increased, whereas the C and O contents decreased. For samples F90 and F100, the F contents on the surface increased significantly, whereas the O contents decreased.

Figure 4 shows the peak-fitting results for the C1s spectra of the fluorinated samples (Figure 3). Figure 5 show the ratio (%) of each bond derived from Figure 4. For sample F10, the ratios of the $\text{C}-\text{O}$, $-\text{CHF}-$, and $-\text{CF}_2-$ bonds were approximately 39%, 38%, and 22%, respectively. As the F_2 gas proportion in the $\text{F}_2\text{-O}_2$ gas mixture increased, the ratio of the $\text{C}-\text{O}$ bond decreased, whereas those of the $-\text{CHF}-$ and $-\text{CF}_2-$ bonds increased. No $-\text{CF}_3$ bond was detected on the sample surface when the F_2 gas proportion in the $\text{F}_2\text{-O}_2$ gas mixture was $<70\%$. In contrast, the ratio of the $-\text{CF}_3$ bond increased significantly when the F_2 gas proportion in the $\text{F}_2\text{-O}_2$ gas mixture was $>90\%$. The formation of strong CF_3 bonds on the surface may influence the wettability with the dye solution. Consequently, the on C-C bonds on the untreated surface were converted into $-\text{C}=\text{O}$ bonds in the form of $-\text{C}(=\text{O})\text{OH}$ groups with moisture in air. In addition, the content of the polar groups ($-\text{CHF}$ and $-\text{CF}_2-$) increased after fluorination.

After surface fluorination, the bonds derived from PP decreased because they were converted into fluorinated $-\text{CF}_x$ bonds, which have high electronegativities according to the zeta potential results (Figure 6). In contrast, the zeta potential at the surface of the

untreated sample was weakly negatively charged. In particular, the zeta potential of sample F30 (-53 mV) was approximately four times higher than that of the untreated sample (-14 mV). This may be attributed to the increase in the number of polar groups (-C-O, -CHF-, and -CF_x) on the samples. The negatively charged surface after fluorination corresponds to previously reported results [21]. However, the effect of F₂ proportion in the mixed gas on the zeta potential did not change significantly. This may be owing to the various polar groups, which includes -CF_x and -C-O bonds.

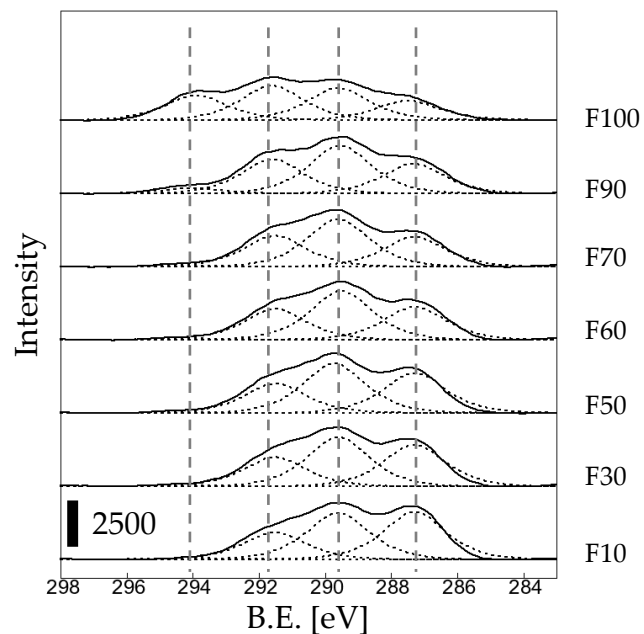


Figure 4. C1s peak separation for the fluorinated samples.

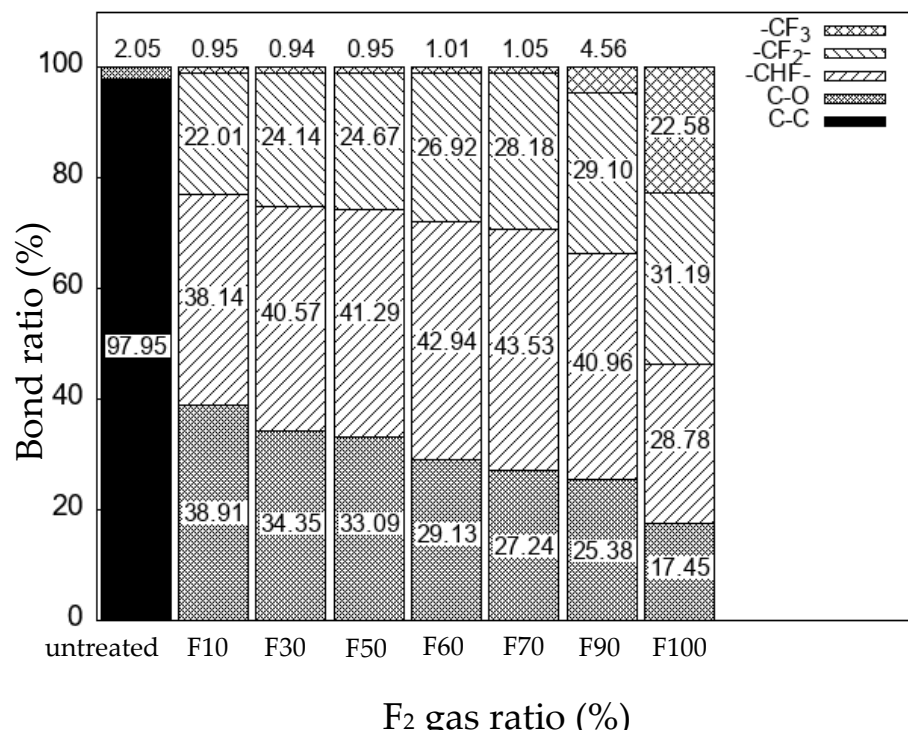


Figure 5. The ratio of the different bonds in the untreated and fluorinated PP samples.

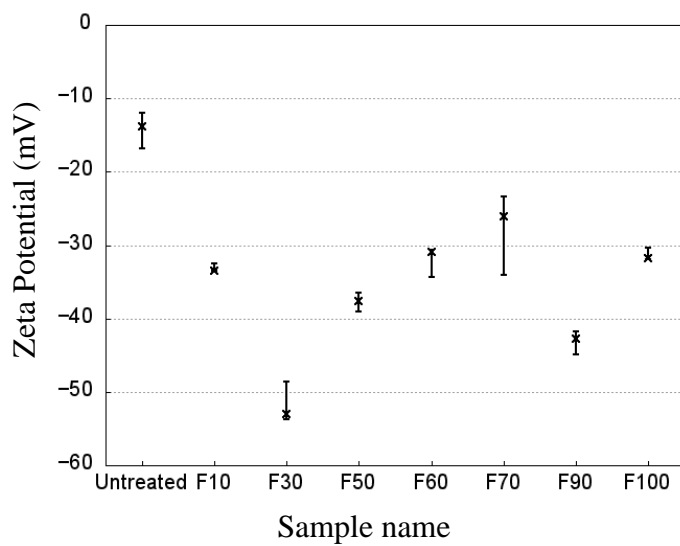


Figure 6. Zeta potential of the untreated and fluorinated PP samples with water at a constant pH of 7.0.

3.3 Dyeing of the surface-modified PP plates

The dye staining of the untreated and fluorinated PP samples are shown in Figure 7. Dyeing tests were performed using (a) O₂ and (b) MB solutions as representative acidic and basic dyes, respectively. No staining was detected in the untreated samples using either dye. Moreover, the fluorinated PP samples were not stained by the acidic O₂ dye. However, the fluorinated PP samples were stained by the basic MB dye, and an increasingly deeper color was observed with increasing F₂ gas proportion in the gas mixture. This is attributed to the surface state of the fluorinated PP samples, which possesses high electronegativity and acidity. In contrast to the O₂ dye, MB has cationic properties that facilitate easy adsorption on the enhanced negative surface of fluorinated PP via Coulombic attraction [25]. Thus, fluorinated PP can be effectively stained with basic dyes, but not acid dyes. However, at F₂ gas proportions of >90%, the dye staining of the PP samples decreased despite the use of the MB solution. This is owing to the formation of hydrophobic -CF₃ bonds in samples F90 and F100, which have higher water contact angles, as shown in Figure 1. Thus, dye staining depends on the surface state of PP, such as the hydrophilicity, roughness, and surface charge. Moreover, dye staining can be controlled by the fluorination conditions.

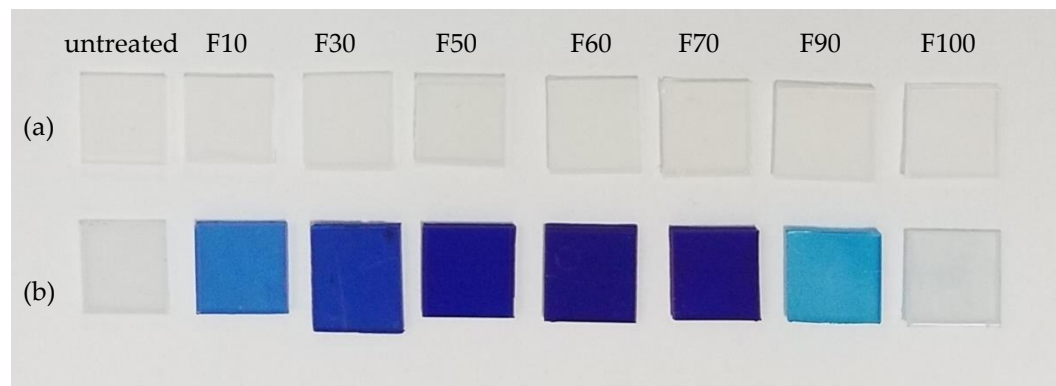


Figure 7. Photographs of the dye staining of the untreated and fluorinated PP samples with (a) orange 2 (O₂) and (b) methylene blue (MB) solutions.

The surface state of the PP samples stained with the MB and O2 dyes was measured using FTIR (Figures 8 and 9). The fluorocarbon peak was detected in all the dyed fluorinated samples. The surface of the fluorinated PP samples were still covered with fluorocarbons after staining. As shown in Figure 8, a peak attributed to aromatic C=C stretching bonds was detected at 1600 cm^{-1} . The surface content of MB on the stained PP surface was determined from the peak area in the FTIR range of $1531\text{--}1685\text{ cm}^{-1}$, and the results obtained by applying a cubic function to the plots are shown in Figure 10. Notably, the depletion of the MB dye after surface staining of the PP samples was evaluated using FTIR (Figure 8). The area of the C=C stretching peak (1600 cm^{-1}) of the fluorinated PP samples was considerably higher than that of the untreated PP sample. In particular, the MB adsorption by fluorinated sample F-60 was approximately 23.7 times higher than that of the untreated sample. However, at F₂ gas proportions of >90%, MB adsorption decreased because of the increased hydrophobicity of the PP surface. Therefore, it is crucial to control the surface state of PP, such as the hydrophilicity and surface charge, to enhance the dyeing of the polymer. Compared to the staining with the basic MB dye, the intensity of the C=C stretching peak at 1600 cm^{-1} in the samples stained with acidic O2 dye decreased, as shown in Figure 9. This may be owing to the negative surface charge of the PP samples.

The surface state before and after staining with MB dye was measured using XPS, as shown in Figure 11. Based on the MB chemical formula ($\text{C}_{16}\text{H}_{18}\text{ClN}_3\text{S}$), the N content of the adsorbed MB was determined from the N 1s peak. Overall, the N 1s peak intensity of the fluorinated PP samples was considerably higher than that of the untreated PP sample. In addition, the N 1s peak intensity was similar for all the fluorinated samples. Based on the results of the C1s peak before (dotted line) and after (solid line) staining with the MB solution, the polar groups (-C-O, -CHF-, and -CF_x) on the PP surface, as shown in Figure 4, decreased significantly and transformed into C-C bonds at 285 eV after MB staining. In addition, the intensity of the F 1s and O 1s peaks decreased and shifted to lower binding energies after MB staining. This may be owing to a substitution reaction between the basic

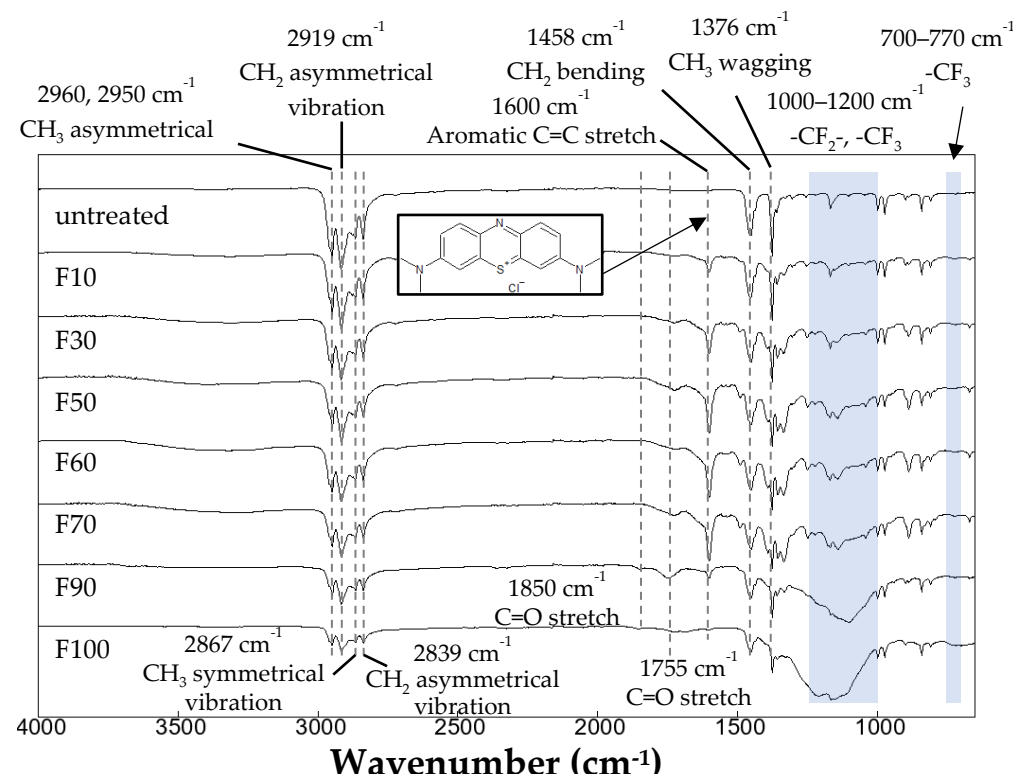


Figure 8. FTIR spectra of the PP samples after dyeing with MB dye.

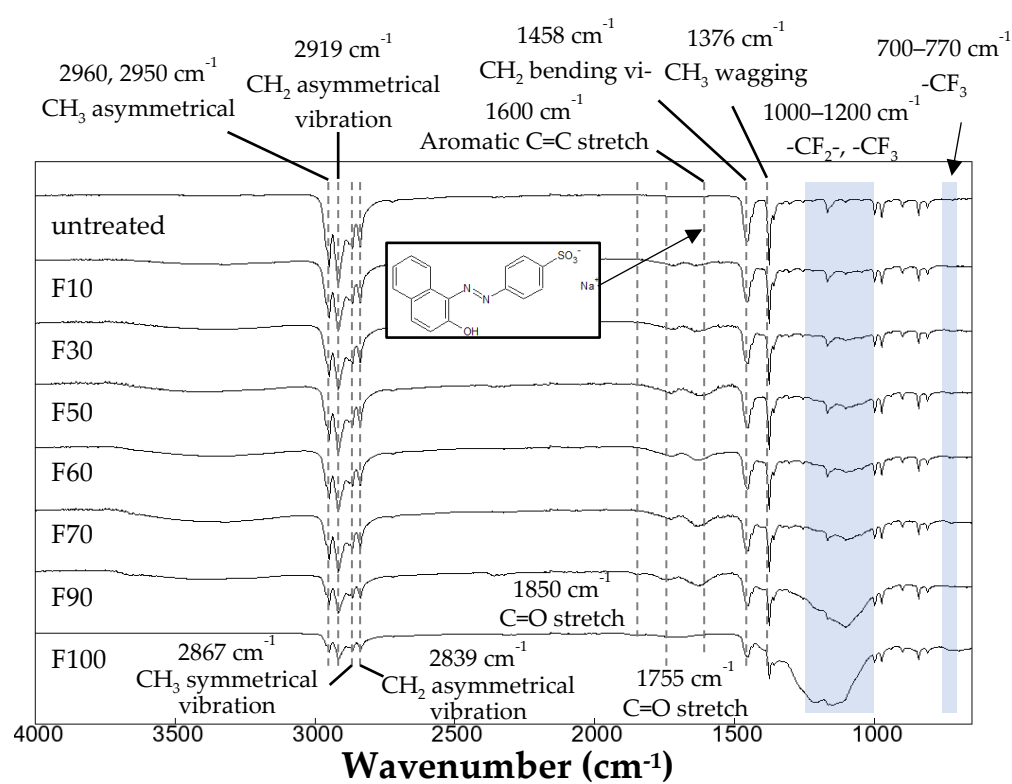


Figure 9. FTIR spectra of the PP samples after dyeing with O₂.

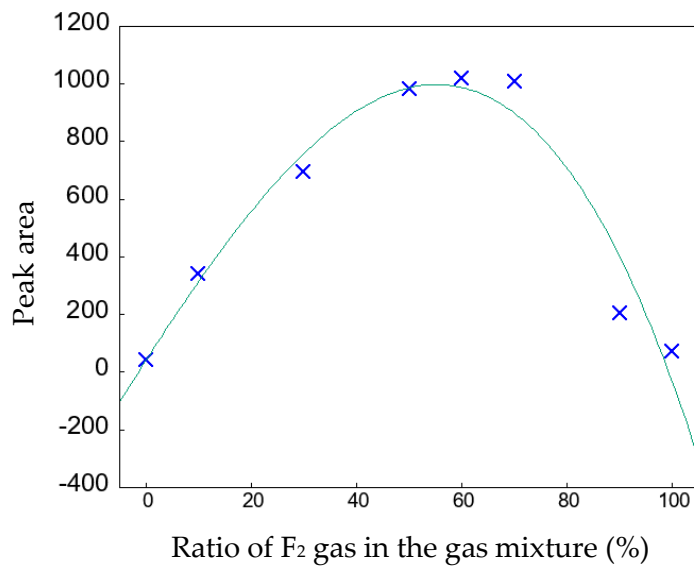


Figure 10. Area of the 1600 cm⁻¹ peak on the MB-dyed PP sample surfaces determined by FTIR (Figure 8).

MB dye and the negatively charged polar groups via Coulombic attraction that occurred In the fluorinated PP samples during MB staining [26].

Although staining the PP resin with dye is difficult, surface fluorination can modify the PP surface into a dyeable surface. The formed fluoride layer has a high surface roughness and negative surface charge, which facilitate the retention of MB molecules. Moreover, it is crucial to maintain the hydrophilic surface and prevent hydrophobic -CF₃ bond

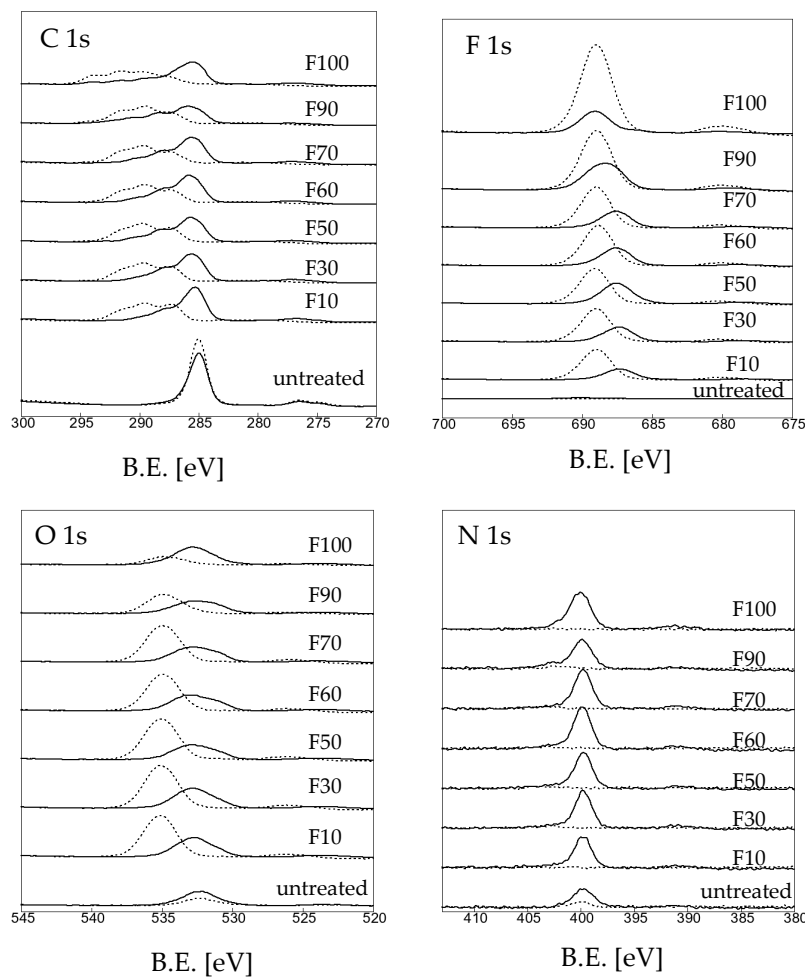


Figure 11. XPS spectra of the PP samples before and after staining with MB dye. Dotted line: before staining, solid line: after staining.

formation. Therefore, in this study, the dyeable surface of PP was controlled by adjusting the mixing ratio of F_2 and O_2 in a gas mixture. Furthermore, the surface modification with F_2 and O_2 mixed gas was beneficial for deep coloring of PP to a greater extent than that observed using pure F_2 gas [21].

4. Conclusions

PP plates were successfully modified by surface fluorination with F_2 and O_2 gas mixtures. Increasing the F_2 proportion in the gas mixture enhanced the peaks associated with fluorinated bonds and weakened the peaks associated with PP. Moreover, it led to increased surface roughness and hydrophilicity of the PP plates. However, at F_2 gas proportion of >90%, the surface became hydrophobic owing to the increase in hydrophobic $-CF_3$ bonds. After surface fluorination, the bonds derived from PP were converted into polar groups ($-C-O$, $-CHF-$ and $-CF_x$), which increased the electronegativity of the surface. During the dyeing test, the fluorinated PP samples stained with the basic MB dye exhibited deep coloring. Thus, PP can be effectively stained using basic dyes, but not acid dyes. This may be attributed to a substitution reaction between the MB dye and fluorine, which enhanced the degree of PP dyeing via Coulombic attraction. However, at F_2 gas proportions of >90%, PP dye staining decreased because of the increased hydrophobic $-CF_3$ bonds. Thus, the enhanced dyeing of the PP resin can be obtained by surface fluorination with a F_2 and O_2 gas mixture. However, it is crucial to maintain a hydrophilic and negatively charged PP surface.

Author Contributions: M.N. conducted the surface fluorination of all the samples and wrote the manuscript. J.K. conducted the XPS analysis of all the samples and contributed to the writing of the manuscript. S.Y. performed the FTIR analysis of all the samples. The manuscript was written with contributions from all the authors. All the authors approved the final version of the manuscript.

Funding: This study was not supported by any external funding.

Institutional Review Board Statement: Not applicable.

Informed Consent Statement: Not applicable.

Data Availability Statement: The data related to this study are all presented in the article.

Acknowledgments: The authors thank Dr. Fumihiro Nishimura for the zeta potential measurements.

Conflicts of Interest: The authors declare no competing financial interest.

References

1. Hirai, S.; Phanthong, P.; Okubo, H.; Yao, S. Enhancement of the surface properties on polypropylene film using side-chain crystalline block copolymers. *Polymers* **2020**, *12*, 2736.
2. Hoff, A.; Jacobsson, S. Thermal oxidation of polypropylene in the temperature range of 120–280 °C. *J. Appl. Polym. Sci.* **1984**, *29*, 465–480.
3. Thakur, V.K.; Vennerberg, D.; Kessler, M.R. Green aqueous surface modification of polypropylene for novel polymer nanocomposites. *ACS Appl. Mater. Interfaces* **2014**, *6*, 9349–9356.
4. Akrman, J.; Prikryl, J. Dyeing Behavior of Polypropylene Blend Fiber. I. Kinetic and thermodynamic parameters of the dyeing system. *J. Appl. Polym. Sci.* **1996**, *62*, 235–240.
5. Geleji, F.; Selim, B.; Szabo, K. Pigmentation of polypropylene fibers. *Faserforschung und Textiltechnik* **1965**, *16*, 395–400.
6. Assmann, K.; Schrenk, V. Develops new vehicle for dyeing polypropylene fibers. *Inter. Fiber J.* **1997**, *12*, 44A.
7. Tengsuwan, S.; Ohshima, M. Supercritical carbon dioxide-assisted electroless nickel plating on polypropylene—The effect of copolymer blend morphology on metal–polymer adhesion, *Journal Supercrit. Fluids* **2014**, *85*, 123–134.
8. Shahidi, S.; Ghoranneviss, M.; Moazzenchi, B. Effect of using cold plasma on dyeing properties of polypropylene fabrics. *Fibers Polym.* **2007**, *8*, 123–129.
9. Hirai, S.; Phanthong, P.; Okubo, H.; Yao, S. Enhancement of the surface properties on polypropylene film using side-chain crystalline block copolymers. *Polymers* **2020**, *12*, 2736–2748.
10. Burkinshaw, S.M.; Froehling, P.E.; Mignanelli, M. The effect of hyperbranched polymers on the dyeing of polypropylene fibres. *Dyes Pigm.* **2002**, *53*, 229–235.
11. Hachim, D.; Brown, B.N. Surface modification of polypropylene for enhanced layer by layer deposition of polyelectrolytes. *J. Biomed. Mater. Res. A* **2018**, *106*, 2078–2085.
12. Walzak, M.J.; Flynn, S.; Foerch, R.; Hill, J.M. UV and ozone treatment of polypropylene and poly (ethylene terephthalate). *J. Adhesion Sci. Technol.* **1995**, *9*, 1229–1248.
13. Tanaka, S.; Naganuma, Y.; Kato, C.; Horie, K. Surface modification of vinyl polymers by vacuum ultraviolet light irradiation. *J. Photopolym. Sci. Technol.* **2003**, *16*, 165–170.
14. Strobel, M.; Jones, V.; Lyons, C.S.; Ulsh, M.; Kushner, M.J.; Dorai, R.; Branch, M.C. A comparison of corona-treated and flame-treated polypropylene films. *Plasmas Polym.* **2003**, *8*, 61–95.
15. Blais, P.; Carlsson, D.J.; Cusulog, G.W.; Wiles, D.M. The chromic acid etching of polyolefin surfaces and adhesive bonding. *J. Colloid Interface Sci.* **1974**, *47*, 636–649.
16. Apel, P.Y.; Orelovich, O.L. Etching of submicron pores in thin polypropylene films irradiated with heavy ions. *Nucl. Tracks Radiat. Meas.* **1991**, *19*, 25–28.
17. Kharitonov, A.P.; Kharitonova, L.N. Surface modification of polymers by direct fluorination: A convenient approach to improve commercial properties of polymeric articles. *Pure Appl. Chem.* **2009**, *81*, 451–471.
18. Kirk, S.; Strobel, M.; Lee, C.; Pachuta, S.J.; Prokosch, M.; Lechuga, H.; Jones, M.E.; Lyons, C.S.; Degner, S.; Yang, Y.; Kushner, M.J. Fluorine plasma treatments of polypropylene films, 1-surface characterization. *Plasma Process. Polym.* **2010**, *7*, 107–122.
19. Kim, J.H.; Namie, M.; Yonezawa, S. Enhanced adhesion between polyethylene terephthalate and metal film by surface fluorination. *Comp. Comm.* **2018**, *10*, 205–208.
20. Kim, J.H.; Mishina, T.; Namie, M.; Nishimura, F.; Yonezawa, S. Effects of surface fluorination on the dyeing of polycarbonate (PC) resin, *J. Coat. Res.* **2021**, *9*, 617–624.
21. Namie, M.; Kim, J.H.; Yonezawa, S. Improving the dyeing of polypropylene by surface fluorination. *Colorants* **2022**, *1*, 121–131.

22. Kim, J.H.; Umeda, H.; Ohe, M.; Yonezawa, S.; Takashima, M. Preparation of pure LiPF₆ using fluorine gas at room temperature. *Chem. Lett.* **2011**, *40*, 360–361.
23. Mohammadiaheri, S.; Jaleh, B.; Mohazzab, B.F.; Eslamipanah, M.; Nasrollahzadeh, M.; Varma, R.S. Greener hydrophilicity improvement of polypropylene membrane by ArF excimer laser treatment. *Surf. Coat. Technol.* **2020**, *399*, 126198.
24. Kobayashi, M.; Nishimura, F.; Kim, J.H.; Yonezawa, S. Dyeable hydrophilic surface modification for PTFE substrates by surface fluorination. *Membranes*, **2023**, *13*, 57–69.
25. Yamaguchi, S.; Minbuta, S.; Matsui, K. Adsorption of the cationic dye methylene blue on anodic porous alumina in sodium dodecyl sulfate solutions. *Langmuir*, **2020**, *36*, 4592–4599.
26. Fumoto, I. Studies on dyeing of polyolefins. (1) Dyeing properties of fluorinated polypropylene fiber. *Sen'i Gakkaishi* **1965**, *21*, 590–597.